Supplemental Data

Determination of the proton environment of the high stability menasemiquinone intermediate in *Escherichia coli* nitrate reductase A by pulsed EPR*

Stéphane Grimaldi[‡1], Rodrigo Arias-Cartin[§2], Pascal Lanciano[‡3], Sevdalina Lyubenova[¶4], Rodolphe Szenes[‡], Burkhard Endeward[¶], Thomas F. Prisner[¶], Bruno Guigliarelli[‡], and Axel Magalon[§]

From the [‡]Unité de Bioénergétique et Ingénierie des Protéines (UPR9036), Institut de Microbiologie de la Méditerranée, CNRS & Aix-Marseille Univ, 13009 Marseille, France, [§]Laboratoire de Chimie Bactérienne (UPR9043), Institut de Microbiologie de la Méditerranée, CNRS & Aix-Marseille Univ, 13009 Marseille, France, [¶] Institut für Physikalische und Theoretische Chemie, Univ Frankfurt, 60438 Frankfurt, Germany

Table of contents

1. Chemical structures of ubiquinone-8, menaquinone-8 and phylloquinone

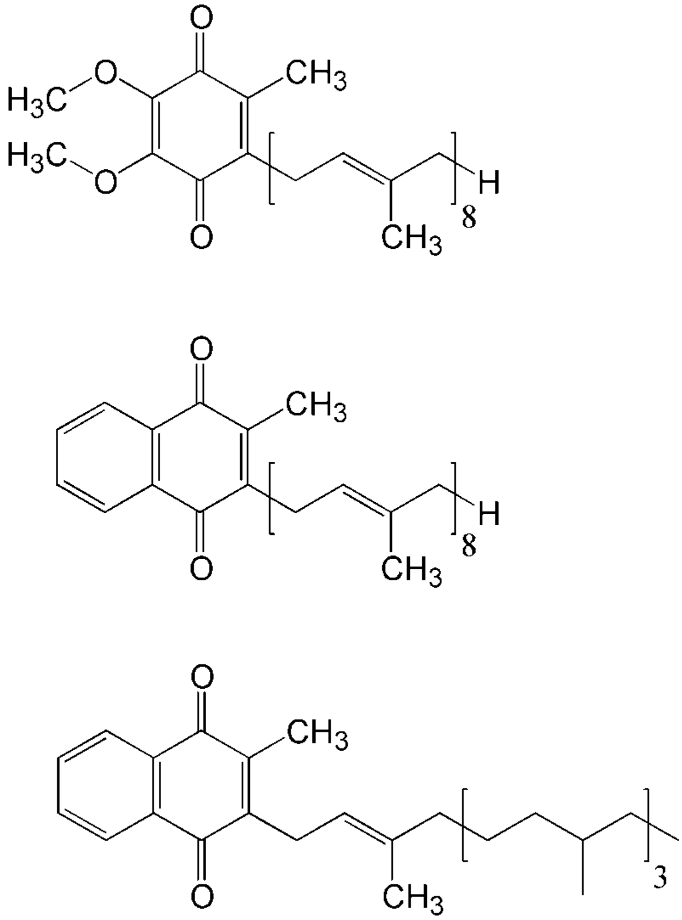

Figure S1. Chemical structures of ubiquinone-8, menaquinone-8 and phylloquinone (from top to the bottom).

2. Analysis of proton HYSCORE spectra

2D-HYSCORE spectra were recorded using the sequence ($\pi/2$ - τ - $\pi/2$ - t_1 - π - t_2 - $\pi/2$), where the inverted three-pulse echo generated at a time τ after the last pulse is measured as a function of t_1 and t_2 (1).

A nucleus with I = ½, such as ^{1}H has two nuclear transition frequencies, ν_α and ν_β, corresponding to two states of the electron spin in the applied magnetic field. In a HYSCORE spectrum, off-diagonal cross-peaks (*i.e.* correlations) (ν_α, ν_β) and (ν_β,ν_α) are created, whose coordinates are nuclear transition frequencies from opposite electron spin manifolds. Orientationally disordered (*i.e.* powder) spectra of I = ½ nuclei (Zeeman frequency ν_I) reveal, in the form of cross-peak contour projections, the interdependence between ν_α and ν_β in the same orientation. In the present analysis, we assume axial symmetry for the hyperfine tensors (2-4). In this case, the hyperfine interactions are determined by two components, $A_\perp$, where the direction of magnetic field is perpendicular to the symmetry axis, and $A_{||}$, where the direction of magnetic field is parallel to the symmetry axis. The correlation patterns in the powder HYSCORE spectrum for axial hyperfine interactions are linear functions in a plot of $\nu^2_{\alpha(\beta)}$ *versus* $\nu^2_{\beta(\alpha)}$ and can be described by Equation S1(5,6):

$$\nu^2_{\alpha(\beta)} = G_{\alpha(\beta)} + Q_{\alpha(\beta)}\nu^2_{\beta(\alpha)} \qquad \text{(Eq. S1)}$$

where the slope $Q_{\alpha(\beta)}$ is

$$Q_{\alpha(\beta)} = (T+2_{Aiso} \mp 4\nu_I)/(T+2A_{iso} \pm 4\nu_I) \qquad \text{(Eq. S2)}$$

and the intercept $G_{\alpha(\beta)}$ is

$$G_{\alpha(\beta)} = \pm 2\nu_I[(4\nu_I^2 - A_{iso}^2 + 2T^2 - A_{iso}T)/(T+2A_{iso} \pm 4\nu_I)] \qquad \text{(Eq. S3)}$$

For each cross-peak, the frequency values along the ridge can be plotted as ν^2_α *versus* ν^2_β and $G_{\alpha(\beta)}$ and $Q_{\alpha(\beta)}$ can be determined by linear fit of plotted data points. These values can then be used to obtain two possible solutions of isotropic (A_{iso}) and anisotropic (T) couplings with the same value of $|2A_{iso}+T|$ and interchanged $|A_\perp| = |A_{iso}-T|$ and $|A_\|| = |A_{iso}+2T|$ (6).

The coordinates (ν_α, ν_β) of arbitrary points along the ridge formed by the lowermost contour for each proton cross-peak were measured from the HYSCORE spectra shown in Figure 2 and plotted as sets of values for ν^2_α *versus* ν^2_β as shown in Figure S2. Fitting of the plotted data points by linear regression gives the slopes and intercepts shown in Table S1. While the larger frequency of each point was arbitrarily selected as ν_β and the smaller was selected as ν_α for peaks 1, 2 and 3, in contrast the opposite assignment of the nuclear frequencies was chosen for peak 4, i.e. $\nu_\beta < \nu_\alpha$. One can see that the points of cross-peaks 4 with the opposite assignment fit the same straight line as the points of peaks 3. This procedure allows one to show that cross-peaks 3 and 4 belong to the same exchangeable proton (H3). Peaks 1 and 2 result from protons H1 and H2. Table S1 shows all possible signs for each set (A_{iso}, T) satisfying Eqs. (S2) and (S3), given that the analysis described in the text provides only relative signs of A_{iso} and T values (4,6,7).

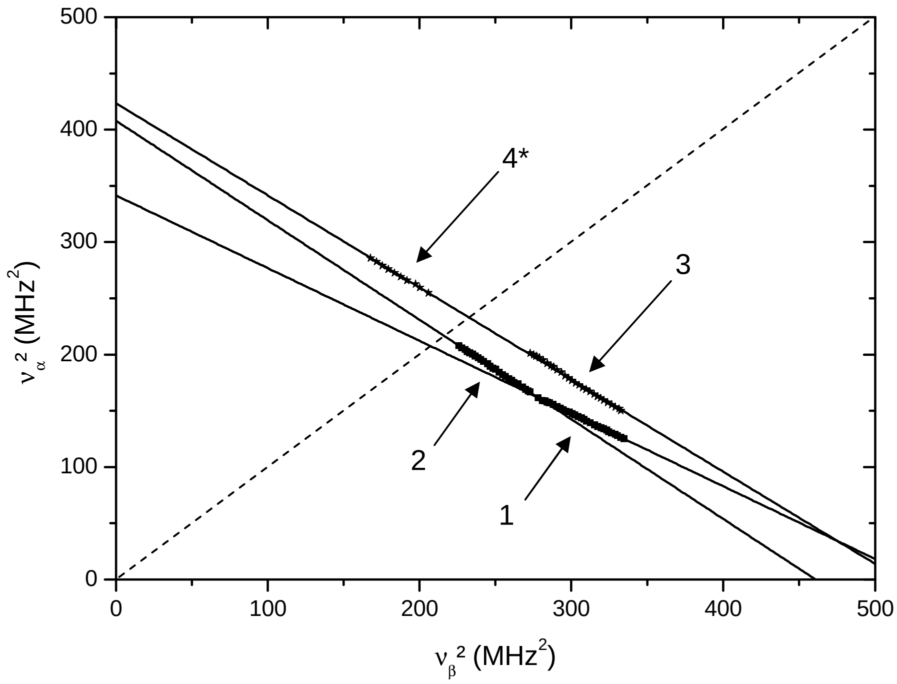

Figure S2. Plots of cross-peaks 1,2,3,4 from HYSCORE spectra (Fig. 2) for MSQ_D in nitrate reductase in the ν^2_α *versus* ν^2_β coordinate system. The straight lines show the linear fit of plotted data points. The dashed line is defined by $\nu^2_\alpha = \nu^2_\beta$ and corresponds to the diagonal in the (++) quadrant of HYSCORE spectra.

Table S1. Parameters derived from contour lineshape analysis of HYSCORE spectra for MSQ_D in NarGHI.

Proton	Q_α	G_α, MHZ^2	(A_{iso},T), MHz
H1 (peaks 1,1')	-0.6539 (0.003)	343.67 (0.70)	$\mp$6.78, ±1.25 ±5.53, ±1.25
H2 (peaks 2,2')	-0.8997 (0.003)	411.42 (0.76)	$\mp$2.14, ±1.18 ±0.96, ±1.18
H3 (peaks 3,3',4,4')	-0.8192 (0.003)	423.37 (0.88)	$\mp$5.79, ±5.73 ±0.06, ±5.73

3. Proton four-pulse ESEEM spectra

In the one-dimensional version of the four-pulse experiment, the time τ between first and second pulses is kept constant and the times $t_1 = t_2$ are increased stepwise. The set of four-pulse envelopes recorded at different τ values forms a blind spot free two-dimensional data set. In powder ESEEM spectra, the frequency of the sum combination harmonic maximum (ν_+) from an I = ½ nucleus (proton in this case) with hyperfine coupling A_{iso} and T is described by Equation (S4) (8):

$$\nu_+ = 2\nu_I\left[1+\frac{9T^2}{16\nu_I^2-(2A_{iso}+T)^2}\right] \qquad \text{(Eq. S4)}$$

One can note that values of $(2A_{iso}+T)^2$ determined for exchangeable protons are significantly less than $16\nu_I(^1H)^2$ (3.46×10^{15} MHz^2 in this case) (Table S2). This means that a simplified equation for the shift $\Delta = \nu_+ - 2\nu_I = 9T^2/16\nu_I$ is applicable in this case and allows for a direct estimation of T from the shift of the sum combination peak from $2\nu_I$.

Table S2. Shift of the frequency of the sum combination harmonic maximum expected in a four-pulse ESEEM spectrum according to the analysis of the HYSCORE spectra.

Proton	(A_{iso},T), MHz	$\lvert 2A_{iso}+T\rvert$ (MHz)	$\lvert 2A_{iso}+T\rvert^2$ (MHz^2)	Δ (MHz)
H1	$\mp$6.78, ±1.25 ±5.53, ±1.25	12.31	1.52e14	0.06
H2	$\mp$2.14, ±1.18 ±0.96, ±1.18	3.1	9.61e12	0.05
H3	$\mp$5.79, ±5.73 ±0.06, ±5.73	5.85	3.42e13	1.26

4. Simulation of the Q-band deuterium Mims ENDOR spectrum

The Q-band ^{2}H Mims ENDOR spectrum shown in Figure 4 was simulated using an isotropic convolutional ENDOR line width of 47 kHz (full width at half maximum). Suppression of signal intensity around the deuterium Larmor frequency known as the central Mims hole, has been explicitly taken into account in the simulation (9). An experimental τ value of 200 ns was chosen as a compromise to get high electron spin echo intensity while having a narrow central Mims hole. A partial orientation selection due to the finite length of the microwave pulses was also included in the simulation.

References

1. Höfer, P., Grupp, A., Nebenführ, H., and Mehring, M. M. (1986) *Chem. Phys. Letters* **132**, 279-284
2. Dikanov, S. A., Samoilova, R. I., Kolling, D. R., Holland, J. T., and Crofts, A. R. (2004) *J. Biol. Chem.* **279**, 15814-15823
3. Yap, L. L., Samoilova, R. I., Gennis, R. B., and Dikanov, S. A. (2006) *J. Biol. Chem.* **281**, 16879-16887
4. Yi, S. M., Narasimhulu, K. V., Samoilova, R. I., Gennis, R. B., and Dikanov, S. A. (2010) *J. Biol. Chem.* **285**, 18241-18251
5. Schweiger, A., and Jeschke, G. (2001) *Principles of pulse electron paramagnetic resonance*, Oxford university press, New York
6. Dikanov, S. A., and Bowman, M. K. (1995) *J. Magn. Reson.* **116**, 125-128
7. Yap, L. L., Samoilova, R. I., Gennis, R. B., and Dikanov, S. A. (2007) *J. Biol. Chem.* **282**, 8777-8785
8. Reijerse, E. J., and Dikanov, S. A. (1991) *J. Chem. Phys.* **95**, 836-845
9. Stoll, S., and Britt, R. D. (2009) *Phys. Chem. Chem. Phys.* **11**, 6614-6625